Analysis of Electric field spatial variability in simulations of electromagnetic waves exposure to mobile telephony base stations

Mame Diarra Bousso Lo-Ndiaye, Nicolas Noé, Pierre Combeau, Yannis Pousset, François Gaudaire

Analysis of Electric field spatial variability in simulations of electromagnetic waves exposure to mobile telephony base stations

Mame Diarra Bousso Lô-Ndiaye[1,2], Nicolas Noé[1], Pierre Combeau[2], Yannis Pousset[2], François Gaudaire[3]
[1] : Centre Scientifique et Technique du Bâtiment, division éclairage et électromagnétisme, Nantes, mame.lo-ndiaye@cstb.fr
[2] : XLIM Institute, UMR CNRS 7252, SIC department, Futuroscope, France, pierre.combeau@univ-poitiers.fr
[3] : Centre Scientifique et Technique du Bâtiment, division éclairage et électromagnétisme, Grenoble, françois.gaudaire@cstb.fr

***Abstract*—this paper focuses on the study of electric field spatial variability in the context of mobile telephony base stations exposure. Electric field is computed using a Uniform Theory of Diffraction (UTD) based simulation technique suitable for large urban areas. Two complementary approaches of spatial variability are proposed here. One based upon spatial autocorrelation and the other one on statistical laws identification to account for electric field distribution in an urban area. The first approach allows us to quantify the spatial dependency of electric field in three representative areas of exposure. The second one demonstrates that statistical laws depending of the area type and urban typology can represent the electric field behavior.**

***Index Terms*—antenna, propagation, measurement, spatial variability.**

I. INTRODUCTION

Numerical simulation is now widely used for rendering of exposure to electromagnetic fields in urban areas characterization, especially in the case of mobile telephony base stations exposure [1,2]. This is due to the ever-increasing power of computation tools and to the quantity and the quality of available topographic data. The results of such simulations have more and more weight as they allow consultation between the public, mobile telephony companies, associations and local communities. They also help to define regulatory methods and as a support to public decision [3]. Nevertheless the high spatial variability of electric field both on a local (around a given exposure point) and a global (in a whole urban area) point of view demands a complete scientific body of work on the presentation of results. Characterizing spatial variability is a major challenge in order to find better indicators of electromagnetic waves exposure.

In this paper we first focus on local spatial variability in three different areas of exposure, depending on emitting and receiving antennas positions. We need to understand how the electric field varies in each of these areas and at which distance this variation becomes significant. We will answer to these questions using spatial autocorrelation analysis with Moran's index.

Then we will analyze the overall behavior of the electric field in a whole urban area by trying to identify statistical laws that effectively accounts for this behavior in the three different areas of exposure. This analysis will be performed on several representative French cities. This study uses the modelisation data from the Copic [3] project funded by the French Ministry of Environment.

As far as areas of exposure are concerned we classify them into three categories:

- Area 1 (A1) where most of the power comes from direct path (in antenna main lobes). The electric field in this area mostly depends on the emitter characteristics.
- Area 2 (A2) where most of the power comes from reflected paths. The electric field in this area also depends on shape and electromagnetic properties of buildings in the vicinity of the emitter.
- Area 3 (A3) where all the power comes only from diffracted paths only. The electric field in this area also depends on the diffraction model and the long range building profile.

The three characteristic areas of exposure are illustrated on Fig. 1.

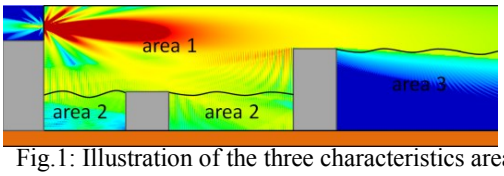

Fig.1: Illustration of the three characteristics areas

These areas are identified on a purely geometric criterion during ray-tracing computation. So, for a given emitter, a receiver is in area 1 if it is in line of sight of the emitter. Otherwise it is in area 2 if there is a reflected path. Other receivers are in area 3, as there always are diffracted paths.

In case of multiple emitters, a receiver is in area 1 if it is in area 1 for at least one of the emitters and so on for areas 2 and 3.

II. LOCAL ANALYSIS OF ELECTRIC FIELD VARIABILITY IN CHARACTERISTIC EXPOSURE AREAS

In this section all the data are computed with the ray-tracing tool MITRA-REM [1].

A. Data description

We look at the spatial variation of the electric field at reception points in each of the exposure areas. The receiver is 1.5m above the ground and receives electric field from a GSM emitter with a 0.16m wavelength. We try to understand how the field behaves around the receiver by taking into account neighborhood within a sphere centered on the receiver, as illustrated on Fig. 2.

Fig.2: Analysis area surrounding the receiver (the receiver is in green and studied samples locations in red)

B. About Moran's index

Spatial autocorrelation is a fundamental concept used in studies of spatial data. This subject has been well explored in the literature [4, 5]. Spatial autocorrelation quantifies likeness between adjacent observations. Many statistical parameters allow quantifying spatial autocorrelation. In particular, Moran's index and Geary's index are the most common ones. According to [6] Moran's index is more robust and less sensitive to local variations. It is a widely used index in geostatistics, statistics and even geographic information systems. Moran's index has also be applied to 3D problems such as image processing [7, 8].

- Mathematical definition

Moran's index is mathematically defined by

$$I = \frac{N \sum_i \sum_j W_{ij} (X_i - \bar{X})(X_j - \bar{X})}{(\sum_i \sum_j W_{ij}) \sum_i (X_i - \bar{X})^2} \quad (1)$$

with W_{ij} is the inverse of the distance between the two observation points i and j, and X_i is the value of the studied variable (electric field here) at observation point i with average value $\bar{X}$. i is the reference index, j is the neighbor index, and N is the total number of reception points in the sample.

Moran's index usually ranges from -1 to 1. The higher the index is, the more likeness between neighbors there is. Strong positive values mean positive spatial autocorrelation (neighbors have similar values). Strong negative values mean negative spatial autocorrelation (neighbors are perfectly dispersed). Values close to zero mean there is no autocorrelation (totally random spatial model).

- Moran's index – hypothesis test

In order to assert Moran's index relevance it must be compared to its theoretical value, using its theoretical average and RMS. In reference [4], Cliff and Ord showed that the theoretical values of average and RMS of Moran's index for null hypothesis (totally random spatial model) are:

$$E(I) = \frac{-1}{N-1} \quad (2)$$

$$\sqrt{V(I)} = \sqrt{\frac{N^2 \Sigma_{ij} Wij^2 + 3 * \left(\Sigma_{ij} Wij\right)^2 - N * \Sigma_i \left(\Sigma_j Wij\right)^2}{(N^2 - 1) * \left(\Sigma_{ij} Wij\right)^2}} \quad (3)$$

Hence Moran's index relevance is tested by computing ZI which is defined by:

$$ZI = \frac{I - E(I)}{\sqrt{V(I)}} \quad (4)$$

ZI is supposed to observe a normal distribution (with an average of 0 and a RMS of 1). The relevance is determined by comparing ZI to its probability p in the table of normal distribution.

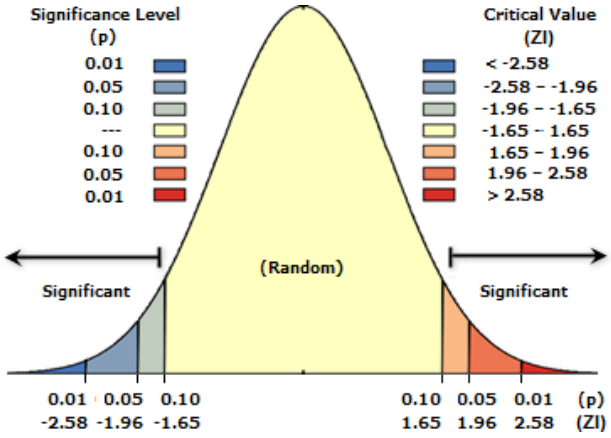

Fig.3 : Abacus to determine the Moran's index relevance

As a consequence a positive (resp. negative) ZI with a low probability p means positive (resp. negative) spatial autocorrelation. The acceptable values for a low probability are illustrated on Fig. 3.

This probability test is only suitable in case of normal distribution of ZI. As a consequence a normality test must be performed. Several tests exist and we used Shapiro-Wilk's one since it is considered as the most reliable and efficient [9, 10] even for a number of samples smaller than 50. We used the R software [11] to achieve the normality test. It is positive if the returned value is greater than a given threshold. A threshold value of 0.1% means that we accept to be wrong in 1 out of 1000 cases when we affirm that the distribution is normal.

C. Results and analysis

The computation of Moran's index is done with a fixed number of samples in the surrounding sphere (*cf.* Fig. 2). The number of neighbors into this sphere must be large enough in order that Moran's index is properly computed, *i.e.* has converged. In our case the radius of the sphere ranges from λ/5 (λ is the wavelength) to 7λ in area 2 and area 3, and to 9λ in area 1. So to find the smallest needed number of receivers to reach the convergence of Moran's index, we studied its relative variation according to the number of receivers within the sphere. We increased the number of receivers until variations of Moran's index become lower than 0.01%. We found that whatever the radius of the sphere is, the number of neighbors must be greater than:

- ≈ 1000 for A1
- ≈ 250 for A2
- ≈ 50 for A3

Now that Moran's index is accurately computed we study the influence of the radius of the sphere on the spatial variation of the electric field. Concretely we first compute I, then ZI and compare ZI values to p. We also checked that ZI has a normal distribution in the sphere for each of the three areas using Shapiro-Wilk's test with a 0.1% threshold.

Results in Table 1 show that the spatial dependency of the electric field in direct (A1) and reflected (A2) areas lies within

a sphere of 4λ radius. Whether for diffracted area (A3) the dependency is larger, even if there is a minimum ZI. Consequently there is a positive spatial autocorrelation on the whole area. Hence all electric field values of receivers in area 3 are very close.

III. GLOBAL ANALYSIS OF ELECTRIC FIELD VARIATION IN CHARACTERISTIC EXPOSURE AREAS

A. Data description

This study has been conducted on results of large simulations of electromagnetic waves exposure to 2G/3G mobile telephony emitters. First, three cities (Paris XV^{ème}, Saint-Mandé and La Rochelle in France) are used in order to determine statistical laws of electric field. Second, two other cities (Paris XIV^{ème} and Cannes in France) are used as a "blind test" to assess these statistical laws. Electric field is computed 1.5m above the ground and on frontages of buildings. The global exposure is studied by computing the cumulative density function (CDF) of electric field according to each emitter and each of the characteristic exposure areas (full environment, areas 1, 2 and 3). Technologies taken into account are GSM900, GSM1800 and UMTS. On Fig.4, we illustrate the simulation of exposure to the scale of city by MITRA-REM [1].

Table 1: Spatial dependency according to sphere radius

	A1		**A2**		**A3**	
Sphere radius (parts of λ)	ZI	p	ZI	p	ZI	p
1/5	116	0	26.64	0	4.33	0
1/4	115	0	26.31	0	4.28	0
1/3	114	0	25.67	0	4.28	0
1/2	111	0	24.23	0	4.23	0
1	96	0	23.79	0	3.65	0
2	26	0	18.48	0	1.68	0.09
3	8.7	0	7.87	0	2.18	0.03
4	2.6	0.012	2.47	0.01	2.95	0
5	-0.08	0.39	1.24	0.18	3.50	0
6	-0.5	0.29	4.97	0	3.53	0
7	-1.16	0.20	7.67	0	3.65	0
8	1.3	0.16				
9	11.6	0				

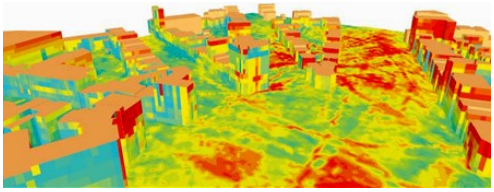

Fig.4: Simulation of the electromagnetic waves exposure by MITRA-REM [1]

B. Methodology

Our aim is to identify a statistical law that efficiently mimics the behavior of the electric field in the three different exposure areas. Since many laws can account for the same variable, we used an in-house tool based upon information criteria [12, 13] so as to select the most relevant law (and its parameters) amongst ten of them using ϕ_β penalty. The lower the criterion is, the most relevant the law is.

C. Results and analysis

The candidate laws are Laplace (Lap), Gamma (Gam), Nakagami (Nak), Normal (Nor), Extreme value (Ev), Weibull (Wei), Lognormal (Log) and Generalized Extreme Value (GEV). Each law is fitted to the simulation results to compute its parameters. We highlight (*Cf.* Table 2) the three best laws that are the most relevant for both ground and frontage exposure, and for the three exposure areas (A1, A2 and A3). The laws are sorted according to the values of the information criterion (according to ϕ_β penalty) given in the tables (the lower the criterion is, the most relevant the law is).

Tables 3, 4, 5 and 6 show that the overall behavior of electric field enforces GEV law, whatever the exposure area and the city are. Even in cases when GEV is not the most relevant law, its penalty is very close to the lower value. The only notable exception is La Rochelle (ground A1) where the best law is Laplace, and GEV is definitely not suitable.

Table 2: Highlighting principle of the best representative laws

Frontage	Ground
L1 (best law)	L1 (best law)
L2 (second best)	L2 (second best)
L3 (third best)	L3 (third best)

Table 3: Results of global analysis into the full environments

Full environment		Saint-Mandé	Paris15	La-Rochelle
Lap	Frontage	1.7080e7	4.2771e6	1.0814e7
	Ground	3.2666e6	6.0913e5	8.7899e5
Gam	Frontage	1.6722e7	4.1450e6	1.0629e7
	Ground	3.1216e6	5.8649e5	8.6973e5
Nak	Frontage	1.6658e7	4.1426e6	1.0579e7
	Ground	3.1434e6	5.9265e5	8.8224e5
Nor	Frontage	1.6644e7	4.1599e6	1.0600e7
	Ground	3.1858e6	6.0645e5	9.0162e5
Ev	Frontage	1.6835e7	4.2568e6	Inf
	Ground	3.3222e6	6.4262e5	1.0329e6
Wei	Frontage	1.8206e7	4.4013e6	1.0988e7
	Ground	3.2706e6	5.9734e5	9.0503e5
Log	Frontage	1.6828e7	4.1603e6	1.0755e7
	Ground	3.1096e6	5.8443e5	8.6783e5
GEV	Frontage	1.6635e7	4.1400e6	1.0616e7
	Ground	3.1061e6	5.8416e5	8.6640e5

Table 4: Results of global analysis into the A1 area

A1		Saint-Mandé	Paris XV^{ème}	La-Rochelle
Lap	Frontage	4.6689e6	1.9450e6	4.5713e6
	Ground	1.4432e6	3.8572e5	5.6677e5
Gam	Frontage	4.6322e6	1.9338e6	3.7521e5
	Ground	1.4418e6	3.7521e5	4.5399e6
Nak	Frontage	4.6434e6	1.9399e6	3.7605e5
	Ground	1.4447e6	3.7605e5	4.5397e6
Nor	Frontage	4.6682e6	1.9532e6	3.7981e5
	Ground	1.4516e6	3.7981e5	4.5722e6
Ev	Frontage	4.9353e6	2.0734e6	4.0515e5
	Ground	1.5549e6	4.0515e5	4.8973e6
Wei	Frontage	5.2500e6	2.1439e6	3.9592e5
	Ground	1.6998e6	3.9592e5	4.7534e6
Log	Frontage	4.6380e6	1.9366e6	3.7733e5
	Ground	1.4472e6	3.7733e5	4.5833e6
GEV	Frontage	4.6311e6	1.9326e6	3.7496e5
	Ground	1.4411e6	3.7496e5	4.5320e6

Table 5: Results of global analysis into the A2 area

A2		Saint-Mandé	Paris XV^{ème}	La-Rochelle
Lap	Frontage	3.5645e6	7.6050e5	2.6838e6
	Ground	5.1472e5	9.4861e4	1.2732e5
Gam	Frontage	3.5362e6	7.4902e5	2.6636e6
	Ground	5.0987e5	9.1545e4	1.2746e5
Nak	Frontage	3.5185e6	7.4685e5	2.6568e6
	Ground	5.0882e5	9.1475e4	1.2638e5
Nor	Frontage	3.5112e6	7.4676e5	2.6600e6
	Ground	5.0980e5	9.2441e4	1.2587e5
Ev	Frontage	3.5958e6	7.6807e5	2.7933e6
	Ground	5.3097e5	9.6111e4	1.2897e5
Wei	Frontage	3.9650e6	8.5083e5	2.9611e6
	Ground	5.6147e5	9.3261e4	1.3588e5
Log	Frontage	3.5679e6	7.5405e5	2.6841e6
	Ground	5.1346e5	9.2422e4	1.2951e5
GEV	Frontage	3.5241e6	7.4636e5	2.6613e6
	Ground	5.0890e5	9.1588e4	1.2623e5

Table 6: Results of global analysis into the A3 area

A3		Saint-Mandé	Paris XV^{ème}	La-Rochelle
lap	Frontage	6.4621e6	9.8425e5	2.3257e6
	Ground	6.7825e5	4.9973e4	1.1765e5
gam	Frontage	6.4175e6	9.8550e5	2.3164e6
	Ground	6.7448e5	4.9735e4	1.1755e5
Nak	Frontage	6.3904e6	9.7831e5	2.3128e6
	Ground	6.6993e5	4.9323e4	1.2116e5
Nor	Frontage	6.3754e6	9.7256e5	2.3180e6
	Ground	6.6776e5	4.9084e4	1.2557e5
Ev	Frontage	6.5376e6	9.8097e5	Inf
	Ground	6.8504e5	4.9962e4	1.3991e5
Wei	Frontage	7.4974e6	1.1635e6	2.5696e6
	Ground	7.3852e5	5.4480e4	1.2224e5
Log	Frontage	6.4630e6	9.9621e5	2.3339e6
	Ground	6.8294e5	5.0490e4	1.1562e5
GEV	Frontage	6.4126e6	9.7467e5	2.3265e6
	Ground	6.7061e5	4.9077e4	1.14772e5

CDF of the adopted laws GEV(5), Lap(6), Nor(7):

$$F(\mu,\sigma,\xi) = exp\left\{\left[1+\xi\left(\frac{x-\mu}{\sigma}\right)\right]\right\}^{\frac{-1}{\xi}} \quad (5)$$

$$F(\mu,b) = \frac{1}{2}\left[1+sgn(x-\mu)\left(1-exp\left(-\frac{|x-\mu|}{b}\right)\right)\right] \quad (6)$$

$$F(\mu,\sigma) = \frac{1}{2}\left(1+\text{erf}\left(\frac{x-\mu}{\sigma\sqrt{2}}\right)\right) \quad (7)$$

Furthermore the parameters of the laws, determined by the algorithm presented in section III.B., are rather similar according to each city, for ground and frontages, as shown on Table 7 for full environment and A1, and on Table 8 for A3.

Table 7: Parameters of the GEV law

City	Frontage	Ground
Full environment		
Saint-Mandé	-0.23 ---10 ---39	0.06---7---35.022
Paris XV^{ème}	-0.12---9.61---30	0.099---6.18---14.4
La-rochelle	-0.09---8.1---21.56	0.008---7.11---19
A1		
Saint-Mandé	-0.11 ---6.80 ---29	0.06---7---35.022
Paris XV^{ème}	-0.10---6.31---24	0.099---6.18---14.4
La-rochelle	-0.10---5.94---16	GEV not suitable

Table 8: Parameters of the Nor law

City area A3 Nor	Frontage	Ground
Saint-Mandé	34 ---6	23---6
Paris XV^{ème}	33---6	21---5

Even if we found that GEV is suitable for A3 area, since it is very close to be the best law, the better law is in fact the Normal law. Once again, like GEV, the parameters of the Normal law are very similar.

D. Validation

The analysis of simulation data demonstrates that the electric field in a city could be duplicated on a city scale for A1, A2 and A3 areas, using GEV. The sole exception is La Rochelle in area A1 (ground). The reason for this exception might be that the La Rochelle city in on the sea-side, and that a lot of ground exposure might be irrelevant (in the sea). In this section we will validate these results by comparing the previous CDF to the ones for two more cities: Paris XIV and Cannes. We show some results of comparisons between simulation and previously computed laws on Fig. 5: Paris XIV frontages in area A1 (a), Paris XIV frontages in area A2 (b) and Cannes ground exposure in area A3 (c).

Paris XIV frontages A1 (a)

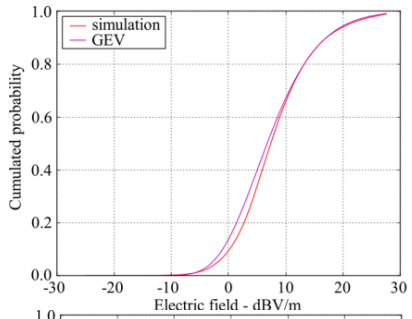

Paris XIV frontages A2 (b)

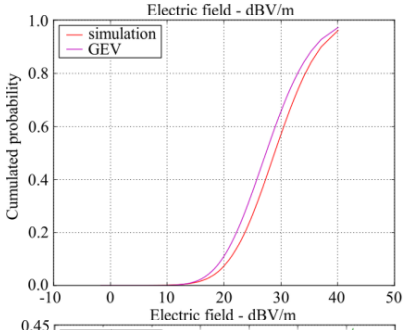

Cannes ground A3 (c)

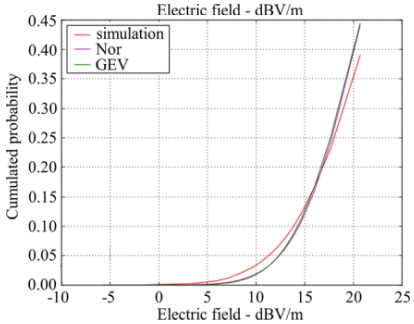

Fig.5: Comparison of the simulated CDF and CDF of the adopted laws

These results fit well to previously found laws. As a consequence these laws allow to faithfully represent electric field distribution on a city scale.

IV. CONCLUSION

The studies presented in this paper allowed characterizing the spatial variation of electric field exposure in different representative areas.

First we quantified the spatial dependency of electric field for a receiver in each of the three exposure areas, showing that each area has a specific stationnarity range. Second we showed that the overall exposure of a city can be represented by general purpose statistical laws. Additional cities should be simulated in order to consolidate these conclusions. In brief this study improved knowledge of electric field behavior. Future work will focus on mixing these results with simulations to be able to have very large scale results by only really computing in restricted areas, in order to have very fast results or to override missing information.

REFERENCES

[1] N. Noé, F. Gaudaire, M. Diarra Bousso Lo, “Estimating and Reducing Uncertainties in Ray-Tracing Techniques for Electromagnetic Field Exposure in Urban Areas”, 2013. Proceedings of IEEE Conference on Antennas and Propagation in Wireless Communications, Torino, Italia. http://geomod.fr/

[2] P. Combeau, L. Aveneau, R. Vauzelle, Y. Pousset, “Efficient 2-D ray-tracing method for narrow and wideband channel characterisation in microcellular configurations”, IEE Proccedings on Microwave Antennas and Propagation, 2006, 153, 502-509.

[3] http://www.developpement-durable.gouv.fr/IMG/pdf/rapport_COPIC_31_juillet_2013.pdf

[4] A.D Cliff, J.K Ord,“Spatial Autoccorrelation”,1973. Londres, Pion

[5] A.D Cliff, J.K Ord,“Spatial Processes:Models and Applications”,1981. Londres, Pion

[6] N Levine,”CrimeStat II: A Spatial Statistics Program for the Analysis of Crime Incident Locations”,2004. Houston/Washington DC, Ned Levine & Associates/the National Institute of Justice

[7] T-J Chen et al, “A novel image quality index using Moran I statistics”,2003, in press

[8] E.C Dasilva ,A.C Silva, A.C de Paiva, R.A Nunes,”Diagnosis of lung nodule using Moran’s index and Geary’s coefficient in compterized tomography images”,2007,in press

[9] J.P Royston, “An extension of Shapiro and Wilk W test for normality to large samples”,1982, Appl. Stat., 31,115 – 124

[10] R Palm,” Macros MiniTable pour la Régression Linéaire,SIMa”, 2002. Faculty of Agricultural Sciences of Gembloux

[11] J Chambers et al, Lucent Technologies, http://www.r-project.org/

[12] O. Alata, C. Olivier, Y. Pousset. “Law recognitions by information criteria for the statistical modeling of small scale fading of the radio mobile channel”, Signal Processing 93, 5 (2013) 1064-1078.

[13] C. Pereira, G. Coq, X. Li, Y. Pousset, C. Olivier, O. Alata, R. Vauzelle, M. Arnaudon, P. Combeau “Application of Information Criteria for the Selection of the Statistical small scale Fading Model of the Radio Mobile Channel”, Elsevier - AEÜ - International Journal of Electronics and Communications – DOI : 10.1016/j.aeue.2009.03.005, 10 pages – 2009